

Observational Constraints on the Parameters of Hořava-Lifshitz Gravity

Himanshu Chaudhary,^{1,2,*} Ujjal Debnath,^{3,†} Shibesh Kumar Jas
Pacif,^{2,‡} Niyaz Uddin Molla,^{3,§} G.Mustafa,^{4,5,¶} and S. K. Maurya^{6,**}

¹*Department of Applied Mathematics, Delhi Technological University, Delhi-110042, India*

²*Pacif Institute of Cosmology and Selfology (PICS), Sagara, Sambalpur 768224, Odisha, India*

³*Department of Mathematics, Indian Institute of Engineering Science and Technology, Shibpur, Howrah-711 103, India*

⁴*Department of Physics, Zhejiang Normal University, Jinhua 321004, Peoples Republic of China*

⁵*New Uzbekistan University, Mustaqillik ave. 54, 100007 Tashkent, Uzbekistan*

⁶*Department of Mathematical and Physical Sciences, College of Arts and Sciences,
University of Nizwa, Nizwa 616, Sultanate of Oman.*

This study investigates the accelerated cosmic expansion within the Hořava-Lifshitz Model. To constrain the cosmological parameters of this model, we incorporate 17 Baryon Acoustic Oscillation points, 31 Cosmic Chronometer points, 40 Type Ia Supernovae points, 24 quasar Hubble diagram points, and 162 Gamma Ray Bursts points, along with the latest Hubble constant measurement (R22). We treat r_d as a free parameter to extract H_0 and r_d using late-time datasets, aiming for optimal fitting values in each model. Treating r_d as free improves precision, reduces bias, and enhances dataset compatibility. The obtained values of H_0 and r_d are compared to the Λ CDM model, showing consistency with previous estimates from Planck and SDSS studies. The Akaike Information Criterion (AIC) and Bayesian Information Criterion (BIC) favor the Hořava-Lifshitz model, with the Λ CDM model having the lowest AIC. Additionally, we conduct Δ AIC and Δ BIC analyses to assess model preference. Validation using the reduced χ^2_{red} statistic indicates satisfactory fits for the Hořava-Lifshitz model, while recognizing Λ CDM as the preferred model. Extensions of the analysis warrant further investigation.

I. INTRODUCTION

Einstein's General theory of relativity (GR) remains the current gold standard for gravitational theories, consistently passing all tests to date [1–3]. Nevertheless, it is important to develop new theories to further test GR and to explore the potential for a theory of gravity beyond GR. Current research interests include finding a valid theory of quantum gravity and explaining cosmological phenomena such as dark energy and dark matter [4–6]. One challenge with GR is that it is not power-counting renormalizable. To address this, Hořava proposed a theory of gravity beyond GR that is both renormalizable and ultraviolet complete [7]. This theory, known as Hořava-Lifshitz (HL) gravity, breaks Lorentz invariance in the ultraviolet regime by introducing a Lifshitz-type anisotropic scaling between space and time.

In Einstein's gravitational theory, a prominent challenge arises from ultraviolet (UV) divergence, known as the UV completion problem. Stelle (1976) addressed this by proposing the incorporation of higher-order curvature invariants into gravitational theories [8]. However, this approach encountered difficulties due to the appearance of ghost degrees of freedom associated with higher-order

derivatives. Horava (2009) effectively tackled this issue by introducing additional terms featuring higher-order spatial curvature components into the action, leading to what is now termed deformed HL gravity [9]. Under high-energy conditions, HL gravity is formulated by abandoning Lorentz symmetry through a Lifshitz-type rescaling process [10]. This rescaling involves altering the scaling properties of space and time coordinates, characterized by an exponent denoted as z , and d representing the spacetime dimension. Lorentz symmetry is broken when $z \neq 1$ and restored only when $z = 1$. Modified HL gravity has garnered significant attention in scientific literature [11–17]. Researchers have explored various aspects, including cosmological implications, such as the Friedmann equation within the deformed HL gravity framework for the FLRW Universe [18], novel approaches to dark energy like holographic dark energy (HDE) [19], and investigations into black hole properties such as quasi-normal modes [20]. Additionally, studies have delved into models involving ghost dark energy within the context of deformed HL gravity [21]. The HL gravity model has been extensively examined by numerous researchers [22–28], exploring its diverse implications and applications across cosmology and gravitational physics.

HL gravity represents a significant endeavor in theoretical physics, aiming to address the quantum gravity problem and rectify the lack of renormalizability inherent in standard general relativity. By providing a UV-complete theory, it seeks to offer a framework capable of describing gravitational interactions at both small quantum scales and large cosmological scales.

* himanshuch1729@gmail.com

† ujjaldebnath@gmail.com

‡ shibesh.math@gmail.com

§ niyazuddin182@gmail.com

¶ gmustafa3828@gmail.com

** sunil@unizwa.edu.om

Despite its ambitious goals, the theory has not been without challenges and criticisms. One major point of contention revolves around its viability as a quantum theory. Critics have raised concerns about the presence of ghost instabilities, which can lead to inconsistencies and unpredictability within the theory's predictions. These challenges have spurred ongoing debate within the scientific community regarding the feasibility and robustness of HL gravity as a fundamental theory of gravity. Nevertheless, researchers remain engaged in studying and refining the HL gravity framework, particularly in its implications for cosmology and black hole physics. Understanding the cosmological consequences of this theory is of particular interest, as it may offer insights into the nature of the universe at large scales. Investigations into black hole properties within this framework also hold promise for elucidating fundamental aspects of gravitational physics. It's important to recognize that the scientific community's understanding of HL gravity is dynamic and subject to change as further research and experimental data become available. Jawad et al. [29] investigated the dynamical stability and cosmographic characteristics of some cosmic models under deformed HL gravity, matching their results with observational data. They studied cosmographic parameters and thermodynamics with regard to Einstein's gravity and deformed HL gravity associated with Kaniadakis HDE [30]. Additionally, they explored the cosmological consequences of Sharma-Mittal holographic dark energy (SMHDE), analysing cosmological parameters and thermodynamics [31]. Further, constraining a model with observations is crucial for ensuring its physical relevance and predictive power. Observational constraints help in refining theoretical models by aligning them with empirical data, thus validating or refuting theoretical predictions. Following the theoretical formulation of HL gravity, various datasets were used by [32] to constrain the corresponding cosmological scenarios. Additionally, [33] focused on the running parameter λ of HL gravity, which governs the flow between the Ultra-Violet and the Infra-Red. They found that λ is restricted to $|\lambda - 1| \lesssim 0.02$, with the best fit value being $|\lambda_{b.f.} - 1| \approx 0.002$. This observational analysis confines the running parameter λ very close to its IR value of 1. It is important to note that basic versions of HL gravity may encounter perturbative instabilities, as highlighted in previous studies [34, 35]. These instabilities pose challenges to the theory's robustness and reliability. Recognizing and addressing these issues is essential for advancing HL gravity and ensuring its consistency with empirical observations and theoretical expectations.

Motivated by the preceding discourse, this study explores into the realm of HL gravity, which emerges as a compelling alternative to Einstein's gravitational theory for several reasons. Both theories aim to describe the behavior of gravity, but they approach the challenge from different perspectives and with different goals in

mind. One key motivation for considering HL gravity over Einstein gravity lies in addressing the UV completion problem, a significant challenge in theoretical physics. HL gravity offers a promising avenue for resolving UV divergences by introducing higher-order spatial curvature components into the action, thereby providing a UV-complete theory capable of describing gravitational interactions at both small quantum scales and large cosmological scales. Our primary objective is to meticulously evaluate the compatibility of HL model with observational data, thus deriving rigorous constraints on crucial cosmic parameters.

Harnessing recent measurements of the Hubble parameter, $H(z)$, extracted from cosmic chronometers, alongside a diverse array of datasets spanning Type Ia Supernovae, Gamma-Ray Bursts (GRB), Quasars, and uncorrelated Baryon Acoustic Oscillations (BAO), our analysis offers a comprehensive survey of the cosmic terrain. Additionally, we aim to probe the ongoing cosmological tensions such as H_0 and the sensitivity of r_d . The paper is structured as follows: In Section II, we present the basic equations of HL Gravity. In Section III, we focus on the methodology employed to constrain the crucial parameters of HL model. Our study's outcomes are detailed in Section IV, where we present the results obtained. Finally, in Section V, we conclude the paper, offering discussions on the implications and significance of our findings.

II. HOŘAVA-LIFSHITZ GRAVITY AND BASIC EQUATIONS

We assume the Arnowitt-Deser-Misner decomposition, which is provided as in the metric form:

$$ds^2 = g_{ij} (dx^i + N^i dt) (dx^j + N^j dt) - N^2 dt^2. \quad (1)$$

In the above equation, N is representing the lapse function, N_i is providing the shift vector, g_{ij} is denoting the spatial metric. For the present analysis, the scaling transformation in the framework of coordinates reads as $t \rightarrow l^3 t$ and $x^i \rightarrow l x^i$. The action of the HL gravity has two major components, namely, the potential term and kinetic term. The HL gravity action within the scope of potential term and kinetic term is defined as:

$$S_g = S_v + S_k = \int dt d^3x \sqrt{g} N (L_v + L_k),$$

where, the kinetic term is defined as

$$S_k = \int dt d^3x \sqrt{g} N \left[\frac{2 (K_{ij} K^{ij} - \lambda K^2)}{\kappa^2} \right],$$

where, The extrinsic curvature is provided as

$$K_{ij} = \frac{\dot{g}_{ij} - \Delta_i N_j - \Delta_j N_i}{2N}.$$

The number of invariants, while working with the Lagrangian, L_v , can be reduced due to its symmetric prop-

erty. This symmetry is referred to as detailed balance. BY using this detailed balance, the action can be revised as

$$S_g = \int dt d^3x \sqrt{g} N \left[\frac{2(K_{ij}K^{ij} - \lambda K^2)}{\kappa^2} + \frac{\kappa^2 C_{ij}C^{ij}}{2\omega^4} - \frac{\kappa^2 \mu \epsilon^{ijk} R_{i,j} \Delta_j R_k^l}{2\omega^2 \sqrt{g}} \right. \\ \left. + \frac{\kappa^2 \mu^2 R_{ij}R^{ij}}{8} - \frac{\kappa^2 \mu^2}{8(3\lambda - 1)} \left\{ \frac{(1 - 4\lambda)R^2}{4} + \Lambda R - 3\Lambda^2 \right\} \right], \quad (2)$$

$$\text{where } C^{ij} = \frac{\epsilon^{ijk} \Delta_k \left(R_i^j - \frac{R}{4} \delta_i^j \right)}{\sqrt{g}}.$$

is the known as the Cotton tensor. Here the covariant derivatives can be determined by the spatial metric $g_{ij}\epsilon^{ijk}$, which is the antisymmetric unit tensor. Here, the parameter λ is the dimensionless constant and the other parameters κ , ω and μ are also the constants.

Horava obtained a gravitational action by consid-

ering the temporal dependency of the lapse function $N(t)$. For FRW metric with the assumptions $N = 1$, $g_{ij} = a^2(t)\gamma_{ij}$, $N^i = 0$ and

$$\gamma_{ij} dx^i dx^j = \frac{dr^2}{1 - kr^2} + r^2 d\Omega_2^2,$$

and by taking the variations of N and g_{ij} , we can obtain the two Field equations which are given below:

$$H^2 = \frac{\kappa^2 \rho_m}{6(3\lambda - 1)} + \frac{\kappa^2}{6(3\lambda - 1)} \left[\frac{3\kappa^2 \mu^2 k^2}{8(3\lambda - 1)a^4} + \frac{3\kappa^2 \mu^2 \Lambda^2}{8(3\lambda - 1)} \right] - \frac{\kappa^4 \mu^2 \Lambda k}{8(3\lambda - 1)^2 a^2}, \quad (3)$$

$$\dot{H} + \frac{3H^2}{2} = -\frac{\kappa^2 p_m}{4(3\lambda - 1)} - \frac{\kappa^2}{4(3\lambda - 1)} \left[\frac{3\kappa^2 \mu^2 k^2}{8(3\lambda - 1)a^4} + \frac{3\kappa^2 \mu^2 \Lambda^2}{8(3\lambda - 1)} \right] - \frac{\kappa^4 \mu^2 \Lambda k}{8(3\lambda - 1)^2 a^2}. \quad (4)$$

where $k = 0, \pm 1$ represent the flat, closed and open universe respectively. In the field equations mentioned above, the term proportional to $\frac{1}{a^4}$ is treated as the "Dark radiation" term and Λ denotes the cosmological constant. Also, $H = \frac{\dot{a}}{a}$ represents the Hubble parameter. Now we assume that the universe is filled with dark matter and we have not taken any external dark energy because the modified gravity can produce dark energy. So the con-

servation equation of the dark matter (DM) is given by

$$\dot{\rho}_m + 3H(\rho_m + p_m) = 0, \quad (5)$$

Since the dark matter has negligible pressure (i.e., $p_m \sim 0$), so the equation (5) yields $\rho_m = \rho_{m0} a^{-3}$. Using the dimensionless parameters $\Omega_{m0} \equiv \frac{\rho_{m0}}{3H_0^2}$, $\Omega_{k0} = -\frac{k}{H_0^2}$, $\Omega_{\Lambda 0} = \frac{\Lambda}{2H_0^2}$, we obtain (choosing $\kappa^2 = 1$)

$$H^2(z) = \frac{2H_0^2 \Omega_{m0} (1+z)^3}{3\lambda - 1} + \frac{\mu^2 H_0^2}{16(3\lambda - 1)^2} [\Omega_{k0} (1+z)^2 + 3\Omega_{\Lambda 0}]^2 \quad (6)$$

III. METHODOLOGY

In our investigation, we carefully picked a specific set of recent Baryon Acoustic Oscillation (BAO) measure-

ments extracted from multiple galaxy surveys, with a primary focus on data from the Sloan Digital Sky Survey (SDSS) [36–41]. To enrich our dataset, we augmented it with valuable contributions from other surveys such

as the Dark Energy Survey (DES) [42], the Dark Energy Camera Legacy Survey (DECaLS) [43], and 6dFGS BAO [44]. Recognizing the potential for interdependencies among our selected data points, we diligently addressed this concern. We carefully curated a subset to mitigate highly correlated points, fully appreciating the importance of managing possible correlations within our chosen dataset. To ensure a comprehensive assessment of systematic errors, we employed mock datasets generated from N-body simulations to precisely calculate covariance matrices. Obtaining accurate covariance matrices among measurements derived from diverse observational surveys presented a significant challenge. To address a significant challenge, we utilized covariance analysis as outlined in reference [45]. Specifically, we adopted the approach where the diagonal elements of the covariance matrix, denoted as C_{ii} , were set equal to the square of the 1σ errors, σ_i^2 . In order to introduce correlations among our selected subset of data, we augmented the covariance matrix by incorporating non-diagonal elements while preserving its symmetry. This was achieved by randomly pairing data points, resulting in a total of twelve pairs. For each pair, the non-diagonal elements were determined using the expression $C_{ij} = 0.5\sigma_i\sigma_j$, where σ_i and σ_j represent the 1σ errors associated with data points i and j , respectively. Through this methodology, we effectively simulated correlations within 56% of the BAO dataset under consideration. This approach enabled us to capture the interdependence among data points, providing a more comprehensive representation of the underlying structure within the dataset. By incorporating these correlations, we aimed to enhance the accuracy and reliability of our analyses, thereby improving our understanding of the phenomenon under investigation. To constrain our cosmological model parameters, we expanded our dataset by including various additional measurements. Firstly, we incorporated thirty independent Hubble parameter measurements derived from cosmic chronometers (CC) detailed in [46–49]. Additionally, our study integrates recent Pantheon Type Ia Supernovae samples [50], 24 binned quasar [51] distance modulus data, 162 Gamma-Ray Bursts (GRBs) [52], and the latest Hubble constant measurement (R22) as an additional prior [53]. To analyze these datasets, we adopted a nested sampling approach using the Polychord package [54], enabling thorough exploration of parameter space for determining optimal fit values. Additionally, we utilized the GetDist package [55] to present our findings clearly and informatively, enhancing the interpretation and visualization of the analysis outcomes. This comprehensive methodology ensures a robust understanding of cosmological parameters while providing insights into the Universe’s fundamental properties.

IV. RESULTS

Fig 1 shows the 68% and 95% confidence levels for important cosmological parameters in the HL Model. The best-fit values for these parameters are listed in Table I. When we incorporate the R22 prior into the Joint dataset, the resulting value for H_0 deviates from the findings in [56], but closely aligns with the SNIe sample in [53]. Conversely, without the R22 priors and using the Joint dataset alone, the estimated value of H_0 aligns more closely with [56]. These findings indicate that the inclusion of the R22 prior diverges from [56] and aligns with [53], showing the impact of prior choice on cosmological parameter estimation. The determined values for the matter density parameter (Ω_{m0}) and (Ω_{d0}) seem lower compared to those documented in [56]. However, this observation aligns with findings from alternative studies [57, 58]. One can observe that the running parameter λ , according to the Joint with R22 analysis, is constrained close to the expected value of 1. Now turning our attention to the Baryon Acoustic Oscillations (BAO) scale, which is a fundamental scale in cosmology derived from the cosmic microwave background, this scale originates from a significant event known as the drag epoch (z_d), marking a pivotal moment when baryons and photons transitioned into distinct entities. The BAO scale (r_d) is essentially a measure of the cosmic sound horizon at z_d , which reflects the separation distance between these baryons and photons. To calculate r_d , we consider the integral of the ratio between the speed of sound (c_s) and the Hubble parameter (H) across a range of redshifts, starting from z_d and extending indefinitely. The speed of sound, c_s , is determined by the fluctuations in pressure (δp_γ) and density ($\delta\rho_B$ and $\delta\rho_\gamma$) within the photon and baryon components. Mathematically, this simplifies to $\frac{1}{\sqrt{3(1+R)}}$, where R represents the ratio of baryon density fluctuations to photon density fluctuations ($R \equiv \frac{\delta\rho_B}{\delta\rho_\gamma} = \frac{3\rho_B}{4\rho_\gamma}$). Observational data, as documented in [56], have provided us with the precise redshift of the drag epoch, $z_d = 1059.94 \pm 0.30$. In the context of a Λ CDM model, the BAO scale r_d has been estimated to be 147.09 ± 0.26 megaparsecs (Mpc) based on measurements by [56]. Fig 2 shows the posterior distribution for the $r_d - H_0$ contour plane of the HL Model. In the HL model, the BAO scale derived solely from BAO datasets is 148.814 ± 10.558 Mpc. Upon including the R22 prior exclusively into the BAO dataset, the sound horizon at the drag epoch becomes 138.907 ± 2.129 Mpc. For the Joint dataset, the BAO scale is 145.843 ± 2.47 Mpc. Integrating the R22 prior into the full dataset yields $r_d = 142.742 \pm 1.658$ Mpc. The findings indicate that when incorporating the joint dataset, the obtained value of r_d in each dark energy model closely agrees with the values obtained in [56]. However, when combining the R22 priors with the joint dataset, the obtained value of r_d aligns closely with [59]. [60] introduces an insightful

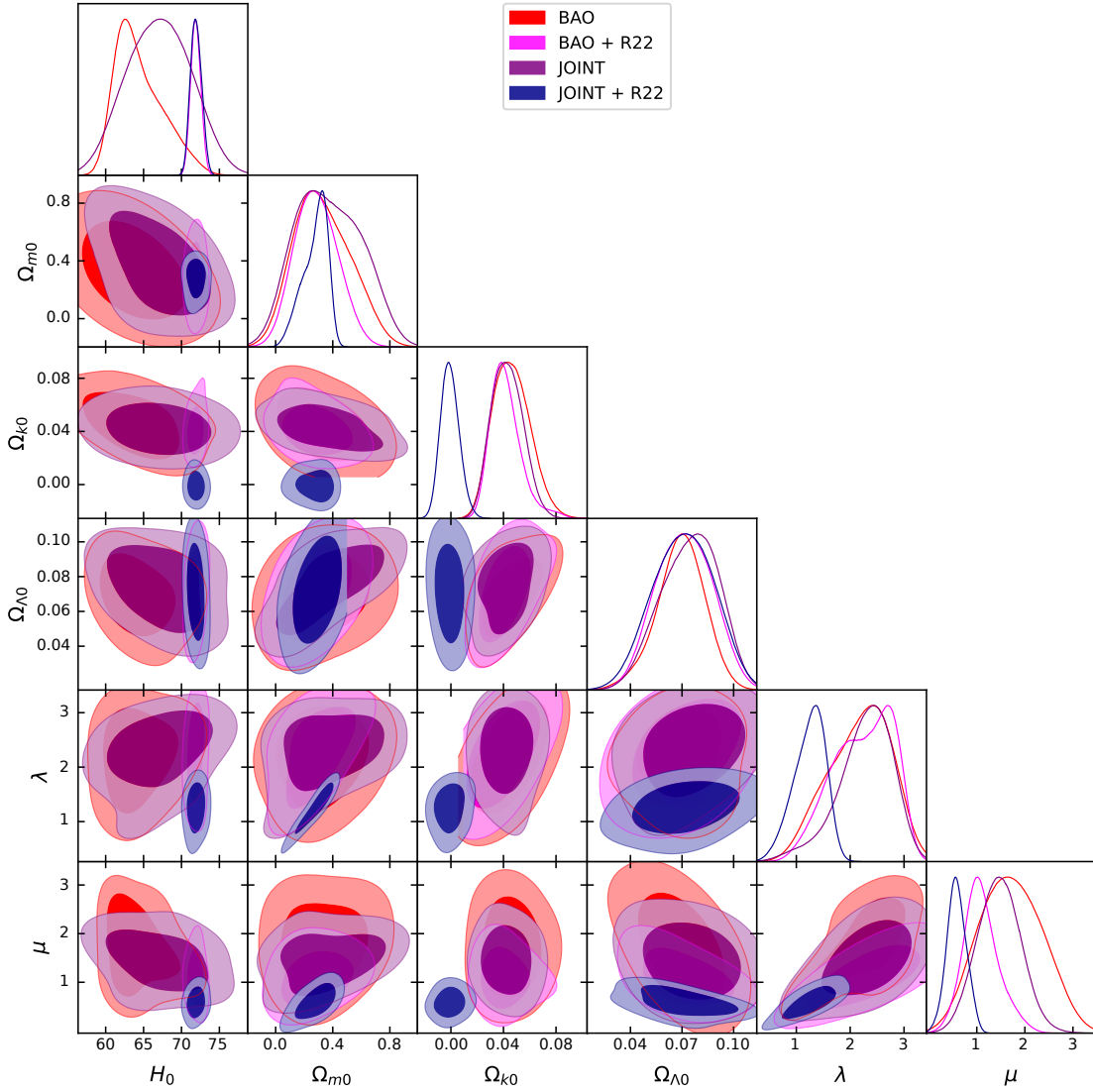


FIG. 1: The figure illustrates the posterior distribution of various observational data measurements using the HL Model, highlighting the 1σ and 2σ regions.

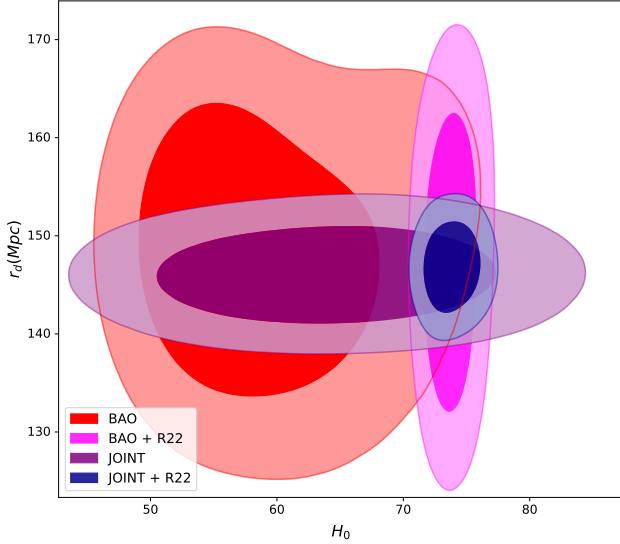
perspective by employing binning and Gaussian methods to amalgamate measurements of 2D BAO and SNIa data. It's important to recognize that the outcomes we derive are closely tied to the initial range of priors we make about the BAO scale (r_d) and the Hubble constant (H_0). These priors significantly impact the values we estimate, particularly when considering the $r_d - H_0$ contour plot. An interesting observation emerges when we omit the R22 prior from our analysis: in such cases, the results for H_0 and r_d tend to better align with findings from the Planck and SDSS experiments.

When assessing various cosmological models, we employ both the Akaike Information Criterion (AIC) [57] and the Bayesian Information Criterion (BIC) for evaluation purposes. The AIC and BIC are statistical measures used to assess the goodness of fit of a model

to a given dataset while penalizing for the number of parameters in the model. The AIC is calculated using the formula: $AIC = -2 \ln(\mathcal{L}_{\max}) + 2k + \frac{2k(2k+1)}{N_{\text{tot}} - k - 1}$. Here, \mathcal{L}_{\max} represents the maximum likelihood of the data, N_{tot} is the total number of data points, and k is the number of parameters in the model. When the total number of data points (N_{tot}) is large, the expression simplifies to: $AIC \simeq -2 \ln(\mathcal{L}_{\max}) + 2k$ which is the conventional form of the AIC criterion. This criterion provides a trade-off between the goodness of fit and the complexity of the model. On the other hand, the BIC is defined as: $BIC = -2 \ln(\mathcal{L}_{\max}) + k \ln N_{\text{tot}}$. The BIC also evaluates the goodness of fit while penalizing for the number of parameters, but it imposes a stronger penalty for additional parameters compared to the AIC, particularly for smaller sample sizes. To

MCMC Results						
Model	Parameter	Priors	BAO	BAO + R22	Joint	Joint + R22
Λ CDM Model	H_0	[50.,80.]	$70.256500^{+9.206346}_{-5.502574}$	$73.798696^{+2.543240}_{-1.315504}$	$69.837362^{+2.478047}_{-1.204873}$	$71.508817^{+1.614354}_{-0.882681}$
	Ω_{m0}	[0.,1.]	$0.270161^{+0.033280}_{-0.013827}$	$0.268255^{+0.043787}_{-0.016790}$	$0.274526^{+0.021367}_{-0.009858}$	$0.270609^{+0.022243}_{-0.009678}$
	$r_d(\text{Mpc})$	[100.,200.]	$145.807497^{+13.994434}_{-9.060325}$	$138.345762^{+4.939114}_{-2.451777}$	$145.811932^{+4.545176}_{-2.347736}$	$142.591327^{+3.951717}_{-1.850175}$
	r_d/r_{fid}	[0.9,1.1]	$0.970661^{+0.068973}_{-0.055989}$	$0.930500^{+0.028238}_{-0.021272}$	$0.974064^{+0.057975}_{-0.033510}$	$0.947662^{+0.043021}_{-0.028335}$
Hořava-Lifshitz Model	H_0	[50.,80.]	$65.700835^{+8.188232}_{-6.213905}$	$73.764424^{+2.238343}_{-1.206257}$	$69.083097^{+13.449031}_{-9.523705}$	$73.841896^{+2.325034}_{-1.470940}$
	Ω_{m0}	[0.,1.]	$0.307520^{+0.374679}_{-0.246232}$	$0.313934^{+0.279260}_{-0.193706}$	$0.301674^{+0.441591}_{-0.290568}$	$0.316901^{+0.251704}_{-0.121592}$
	Ω_{k0}	[0.,0.1]	$0.045949^{+0.019647}_{-0.015391}$	$0.041633^{+0.015582}_{-0.011413}$	$0.042779^{+0.017139}_{-0.013332}$	$-0.000867^{+0.011261}_{-0.006873}$
	$\Omega_{\Lambda 0}$	[0.,0.1]	$0.069321^{+0.031470}_{-0.011309}$	$0.071208^{+0.025913}_{-0.016735}$	$0.074617^{+0.032586}_{-0.017924}$	$0.070843^{+0.032504}_{-0.018968}$
	λ	[0.,1.]	$2.179575^{+1.092257}_{-0.718167}$	$2.250670^{+1.174342}_{-0.613784}$	$2.286921^{+1.402826}_{-0.450757}$	$1.249560^{+0.687458}_{-0.309072}$
	μ	[0.,3.]	$1.709372^{+1.036271}_{-0.696013}$	$1.090299^{+0.706884}_{-0.313413}$	$1.457249^{+0.864455}_{-0.445976}$	$0.581412^{+0.432033}_{-0.201536}$
	$r_d(\text{Mpc})$	[100.,200.]	$148.489236^{+14.876427}_{-8.942271}$	$147.612337^{+13.663930}_{-9.931756}$	$146.021893^{+5.394418}_{-2.757663}$	$146.862925^{+5.019343}_{-3.047961}$
	r_d/r_{fid}	[0.9,1.1]	$1.004965^{+0.099047}_{-0.058313}$	$0.993782^{+0.086915}_{-0.064095}$	$0.979637^{+0.032327}_{-0.020247}$	$0.991474^{+0.034560}_{-0.020670}$

TABLE I: Summary of the MCMC Results.

FIG. 2: The figure illustrates the posterior distribution of various observational data measurements using the HL Model, highlighting the 1σ and 2σ regions.

compare different models, we use the differences in AIC and BIC values, denoted as ΔAIC and ΔBIC , respectively: $\Delta\text{AIC} = \text{AIC}_{\text{HL Model}} - \text{AIC}_{\Lambda\text{CDM Model}}$ and $\Delta\text{BIC} = \text{BIC}_{\text{HL Model}} - \text{BIC}_{\Lambda\text{CDM Model}}$. These differences help to identify the relative performance of models, with lower values indicating a better fit relative to the reference model. The interpretation of ΔAIC and ΔBIC values is as follows: - ΔAIC or $\Delta\text{BIC} \leq 2$: Substantial evidence for the model. - ΔAIC or ΔBIC between 4 and 7: Considerable evidence against the model. - ΔAIC or $\Delta\text{BIC} \geq 10$: Strong evidence against the model. When comparing the HL Model with the

standard ΛCDM model, it's important to note that both proposed extensions encompass ΛCDM as a subset, differing only by 4 degrees of freedom. This aspect allows for the application of conventional statistical tests. Our evaluation primarily employs the reduced chi-square statistic, denoted as $\chi^2_{\text{red}} = \chi^2/\text{Dof}$, where "Dof" represents the degrees of freedom of the model, and χ^2 signifies the weighted sum of squared deviations from the expected values. Based on the provided in Table II, we can conduct a comparative study between the ΛCDM Model and HL Model using the metrics of reduced chi-square (χ^2_{red}), Akaike Information Criterion (AIC), ΔAIC , Bayesian Information Criterion (BIC), and ΔBIC . The reduced chi-square value is a measure of how well the model fits the data. A value closer to 1 indicates a better fit. Both models have χ^2_{red} values close to 1, suggesting that both models fit the data well. However, the ΛCDM Model has a slightly lower χ^2_{red} value, indicating a marginally better fit. In terms of the AIC, the ΛCDM Model scores 277.38, whereas the HL Model scores slightly higher at 279.13, resulting in a ΔAIC of 1.75. This indicates substantial evidence for the HL Model, though it is less favored compared to the ΛCDM Model. For the BIC, the ΛCDM Model has a score of 277.59, while the HL Model has a higher score of 280.51, leading to a ΔBIC of 2.92. This ΔBIC suggests positive evidence against the HL Model, indicating a stronger preference for the ΛCDM Model.

V. CONCLUSIONS

In conclusion, our study focused on investigating the accelerated cosmic expansion in the late Universe within

Model	χ^2_{red}	AIC	Δ AIC	BIC	Δ BIC
Λ CDM Model	0.949	277.38	0	277.59	0
Hořava-Lifshitz Model	0.961	279.13	1.75	280.51	2.92

TABLE II: Summary of χ^2_{red} , AIC, Δ AIC, BIC and Δ BIC

the context of the HL Model. This framework offers an alternative perspective to general relativity by incorporating anisotropic scaling at ultraviolet scales. We analyzed 24 Baryon Acoustic Oscillation (BAO) points, along with 31 uncorrelated data points obtained from Cosmic Chronometers methods. We also incorporated 40 points from Type Ia supernovae, 24 points from the Hubble diagram for quasars, and a substantial dataset consisting of 162 points sourced from Gamma Ray Bursts. Furthermore, our study included the latest measurement of the Hubble constant conducted by R22. Our primary objective was to determine the optimal fitting values for every cosmological parameter within each dark energy model. By treating the sound horizon r_d as a free parameter instead of relying on prior information from the Cosmic Microwave Background (CMB), we gain several benefits. Firstly, it reduces bias by sidestepping potentially restrictive CMB priors, ensuring a more impartial estimation of r_d and other cosmological parameters. Secondly, it enhances precision by allowing late-time data, such as Baryon Acoustic Oscillations (BAO) or Type Ia Supernovae (SNIe), to directly inform the measurement of r_d , leading to more accurate results. Moreover, this approach promotes compatibility between datasets from different cosmic epochs, facilitating a more holistic understanding of the Universe's evolution. We determined H_0 and r_d for the HL Model relative to the Λ CDM model as follows: In the Λ CDM model, our analysis yields $H_0 = 69.828145 \pm 1.009964$ km/s/Mpc and $r_d = 146.826212 \pm 2.201612$ Mpc. In the HL model, we obtain $H_0 = 69.966349 \pm 1.403864$ km/s/Mpc and

$r_d = 145.843487 \pm 2.470309$ Mpc. Importantly, our findings underscore that the values of H_0 and r_d based on low-redshift measurements align with early Planck and SDSS estimations. While both the Λ CDM Model and the HL Model fit the data reasonably well, the Λ CDM Model is preferred based on the statistical criteria provided. The Λ CDM Model demonstrates a marginally better fit with a lower reduced chi-square value and is more strongly supported by both the AIC and BIC measures. The Δ AIC indicates substantial evidence for the HL Model, but it is still less favored compared to the Λ CDM Model. Additionally, the Δ BIC provides positive evidence against the HL Model, reinforcing the stronger preference for the Λ CDM Model for the given dataset. Therefore, the Λ CDM Model is favored over the HL Model. These findings underscore the importance of considering alternative cosmological models beyond the standard framework. While the Λ CDM model remains favored due to its simplicity and good fit, the extensions present viable candidates worthy of further investigation. To achieve a better understanding of the fundamental characteristics and development of the Universe, cosmological models must be continually examined and improved.

ACKNOWLEDGEMENTS

N.U.M would like to thank CSIR, Govt. of India for providing Senior Research Fellowship (No. 08/003(0141)/2020-EMR-I).

-
- [1] C. M. Will, *Theory and experiment in gravitational physics*. Cambridge university press, 2018.
 - [2] E. Berti *et al.*, “Testing General Relativity with Present and Future Astrophysical Observations,” *Class. Quant. Grav.*, vol. 32, p. 243001, 2015.
 - [3] C. M. Will, “The confrontation between general relativity and experiment,” *Living reviews in relativity*, vol. 17, no. 1, pp. 1–117, 2014.
 - [4] B. Jain and J. Khoury, “Cosmological tests of gravity,” *Annals of Physics*, vol. 325, no. 7, pp. 1479–1516, 2010.
 - [5] T. Clifton, P. G. Ferreira, A. Padilla, and C. Skordis, “Modified gravity and cosmology,” *Physics reports*, vol. 513, no. 1-3, pp. 1–189, 2012.
 - [6] K. Koyama, “Cosmological tests of modified gravity,” *Reports on Progress in Physics*, vol. 79, no. 4, p. 046902, 2016.
 - [7] P. Horava, “Quantum Gravity at a Lifshitz Point,” *Phys. Rev. D*, vol. 79, p. 084008, 2009.
 - [8] K. S. Stelle, “Renormalization of higher-derivative quantum gravity,” *Physical Review D*, vol. 16, no. 4, p. 953, 1977.
 - [9] P. Hořava, “Quantum gravity at a lifshitz point,” *Physical Review D*, vol. 79, no. 8, p. 084008, 2009.
 - [10] M. Minamitsuji, “Classification of cosmology with arbitrary matter in the hořava–lifshitz model,” *Physics Letters B*, vol. 684, no. 4-5, pp. 194–198, 2010.
 - [11] J. I. Radkovski and S. M. Sibiryakov, “Scattering amplitudes in high-energy limit of projectable horava gravity,” *arXiv preprint arXiv:2306.00102*, 2023.
 - [12] A. Jawad, A. M. Sultan, and S. Rani, “Viability of baryon to entropy ratio in modified hořava–lifshitz gravity,” *Symmetry*, vol. 15, no. 4, p. 824, 2023.

- [13] S. Maity and U. Debnath, “Study of tsallis, rényi and sharma–mittal holographic dark energies for entropy corrected modified field equations in hořava–lifshitz gravity,” *International Journal of Geometric Methods in Modern Physics*, vol. 17, no. 11, p. 2050170, 2020.
- [14] K. Kim, J. J. Oh, C. Park, and E. J. Son, “Neutron star structure in hořava–lifshitz gravity,” *Physical Review D*, vol. 103, no. 4, p. 044052, 2021.
- [15] A. N. Tawfik, A. M. Diab, and E. Abou El Dahab, “Minimal-supersymmetric extended inflation field in horava–lifshitz gravity,” *International Journal of Modern Physics D*, vol. 26, no. 14, p. 1750166, 2017.
- [16] Y. Misonoh, M. Fukushima, and S. Miyashita, “Stability of singularity-free cosmological solutions in hořava–lifshitz gravity,” *Physical Review D*, vol. 95, no. 4, p. 044044, 2017.
- [17] J.-W. Lu, Y.-B. Wu, J. Xiao, C.-J. Lu, and M.-L. Liu, “Holographic superconductors in ir modified hořava–lifshitz gravity,” *International Journal of Modern Physics A*, vol. 31, no. 19, p. 1650110, 2016.
- [18] S.-W. Wei, Y.-X. Liu, and Y.-Q. Wang, “A note on friedmann equation of frw universe in deformed hořava–lifshitz gravity from entropic force,” *Communications in Theoretical Physics*, vol. 56, no. 3, p. 455, 2011.
- [19] A. Jawad and S. Chattopadhyay, “New holographic dark energy in modified $f(r)$ horava–lifshitz gravity,” *Astrophysics and Space Science*, vol. 353, no. 1, pp. 293–299, 2014.
- [20] S. Chen and J. Jing, “Quasinormal modes of a black hole in the deformed hořava–lifshitz gravity,” *Physics Letters B*, vol. 687, no. 2-3, pp. 124–128, 2010.
- [21] A. Sheykhi, S. Ghaffari, and H. Moradpour, “Ghost dark energy in the deformed hořava–lifshitz cosmology,” *International Journal of Modern Physics D*, vol. 28, no. 06, p. 1950080, 2019.
- [22] M. Chaichian, S. Nojiri, S. D. Odintsov, M. Oksanen, and A. Tureanu, “Modified $f(r)$ hořava–lifshitz gravity: a way to accelerating frw cosmology,” *Classical and Quantum Gravity*, vol. 27, no. 18, p. 185021, 2010.
- [23] S. Carloni, M. Chaichian, S. Nojiri, S. D. Odintsov, M. Oksanen, and A. Tureanu, “Modified first-order hořava–lifshitz gravity: Hamiltonian analysis of the general theory and accelerating frw cosmology in a power-law $f(r)$ model,” *Physical Review D*, vol. 82, no. 6, p. 065020, 2010.
- [24] E. Elizalde, S. Nojiri, S. Odintsov, and D. Saez-Gomez, “Unifying inflation with dark energy in modified $f(r)$ hořava–lifshitz gravity,” *The European Physical Journal C*, vol. 70, pp. 351–361, 2010.
- [25] S. Nojiri and S. D. Odintsov, “Covariant renormalizable gravity and its frw cosmology,” *Physical Review D*, vol. 81, no. 4, p. 043001, 2010.
- [26] S. Nojiri and S. D. Odintsov, “A proposal for covariant renormalizable field theory of gravity,” *Physics Letters B*, vol. 691, no. 1, pp. 60–64, 2010.
- [27] S. Nojiri and S. D. Odintsov, “Covariant power-counting renormalizable gravity: Lorentz symmetry breaking and accelerating early-time frw universe,” *Physical Review D*, vol. 83, no. 2, p. 023001, 2011.
- [28] K. Bamba, S. Capozziello, S. Nojiri, and S. D. Odintsov, “Dark energy cosmology: the equivalent description via different theoretical models and cosmography tests,” *Astrophysics and Space Science*, vol. 342, pp. 155–228, 2012.
- [29] A. Jawad and M. Usman, “Some interacting cosmic models in deformed hořava–lifshitz gravity and dynamical stability,” *The European Physical Journal Plus*, vol. 138, no. 1, pp. 1–9, 2023.
- [30] A. Jawad and M. Usman, “Some interacting cosmic models in deformed hořava–lifshitz gravity and dynamical stability,” *The European Physical Journal Plus*, vol. 138, no. 1, pp. 1–9, 2023.
- [31] V. C. Dubey, U. K. Sharma, and A. Pradhan, “Sharma–mittal holographic dark energy model in conharmonically flat space-time,” *International Journal of Geometric Methods in Modern Physics*, vol. 18, no. 01, p. 2150002, 2021.
- [32] S. Dutta and E. N. Saridakis, “Observational constraints on hořava–lifshitz cosmology,” *Journal of Cosmology and Astroparticle Physics*, vol. 2010, no. 01, p. 013, 2010.
- [33] S. Dutta and E. Saridakis, “Overall observational constraints on the running parameter of horava–lifshitz gravity,” *J. Cosmol. Astropart. Phys.*, vol. 2010, p. 013, 2010.
- [34] C. Bogdanos and E. N. Saridakis, “Perturbative instabilities in hořava gravity,” *Classical and Quantum Gravity*, vol. 27, no. 7, p. 075005, 2010.
- [35] C. Charmousis, G. Niz, A. Padilla, and P. M. Saffin, “Strong coupling in hořava gravity,” *Journal of High Energy Physics*, vol. 2009, no. 08, p. 070, 2009.
- [36] A. J. Ross, L. Samushia, C. Howlett, W. J. Percival, A. Burden, and M. Manera, “The clustering of the sdss dr7 main galaxy sample–i. a 4 per cent distance measure at $z = 0.15$,” *Monthly Notices of the Royal Astronomical Society*, vol. 449, no. 1, pp. 835–847, 2015.
- [37] S. Alam, M. Ata, S. Bailey, F. Beutler, D. Bizyaev, J. A. Blazek, A. S. Bolton, J. R. Brownstein, A. Burden, C.-H. Chuang, *et al.*, “The clustering of galaxies in the completed sdss-iii baryon oscillation spectroscopic survey: cosmological analysis of the dr12 galaxy sample,” *Monthly Notices of the Royal Astronomical Society*, vol. 470, no. 3, pp. 2617–2652, 2017.
- [38] H. Gil-Marín, J. E. Bautista, R. Paviot, M. Vargas-Magaña, S. de La Torre, S. Fromenteau, S. Alam, S. Ávila, E. Burtin, C.-H. Chuang, *et al.*, “The completed sdss-iv extended baryon oscillation spectroscopic survey: measurement of the bao and growth rate of structure of the luminous red galaxy sample from the anisotropic power spectrum between redshifts 0.6 and 1.0,” *Monthly Notices of the Royal Astronomical Society*, vol. 498, no. 2, pp. 2492–2531, 2020.
- [39] A. Raichoor, A. De Mattia, A. J. Ross, C. Zhao, S. Alam, S. Ávila, J. Bautista, J. Brinkmann, J. R. Brownstein, E. Burtin, *et al.*, “The completed sdss-iv extended baryon oscillation spectroscopic survey: large-scale structure catalogues and measurement of the isotropic bao between redshift 0.6 and 1.1 for the emission line galaxy sample,” *Monthly Notices of the Royal Astronomical Society*, vol. 500, no. 3, pp. 3254–3274, 2021.
- [40] J. Hou, A. G. Sánchez, A. J. Ross, A. Smith, R. Neveux, J. Bautista, E. Burtin, C. Zhao, R. Scoccimarro, K. S. Dawson, *et al.*, “The completed sdss-iv extended baryon oscillation spectroscopic survey: BAO and rsd measurements from anisotropic clustering analysis of the quasar sample in configuration space between redshift 0.8 and 2.2,” *Monthly Notices of the Royal Astronomical Society*, vol. 500, no. 1, pp. 1201–1221, 2021.
- [41] H. D. M. Des Bourbonx, J. Rich, A. Font-Ribera, V. de Sainte Agathe, J. Farr, T. Etourneau, J.-M.

- Le Goff, A. Cuceu, C. Balland, J. E. Bautista, *et al.*, “The completed sdss-iv extended baryon oscillation spectroscopic survey: baryon acoustic oscillations with ly α forests,” *The Astrophysical Journal*, vol. 901, no. 2, p. 153, 2020.
- [42] T. Abbott, M. Agüena, S. Allam, A. Amon, F. Andrade-Oliveira, J. Asorey, S. Avila, G. Bernstein, E. Bertin, A. Brandao-Souza, *et al.*, “Dark energy survey year 3 results: A 2.7% measurement of baryon acoustic oscillation distance scale at redshift 0.835,” *Physical Review D*, vol. 105, no. 4, p. 043512, 2022.
- [43] S. Sridhar, Y.-S. Song, A. J. Ross, R. Zhou, J. A. Newman, C.-H. Chuang, R. Blum, E. Gaztanaga, M. Landriau, and F. Prada, “Clustering of lrgs in the decals dr8 footprint: Distance constraints from baryon acoustic oscillations using photometric redshifts,” *The Astrophysical Journal*, vol. 904, no. 1, p. 69, 2020.
- [44] F. Beutler, C. Blake, M. Colless, D. H. Jones, L. Staveley-Smith, L. Campbell, Q. Parker, W. Saunders, and F. Watson, “The 6df galaxy survey: baryon acoustic oscillations and the local hubble constant,” *Monthly Notices of the Royal Astronomical Society*, vol. 416, no. 4, pp. 3017–3032, 2011.
- [45] L. Kazantzidis and L. Perivolaropoulos, “Evolution of the $f\sigma_8$ tension with the planck 15/ Λ cdm determination and implications for modified gravity theories,” *Physical Review D*, vol. 97, no. 10, p. 103503, 2018.
- [46] M. Moresco, “Raising the bar: new constraints on the hubble parameter with cosmic chronometers at $z \sim 2$,” *Monthly Notices of the Royal Astronomical Society: Letters*, vol. 450, no. 1, pp. L16–L20, 2015.
- [47] M. Moresco, L. Pozzetti, A. Cimatti, R. Jimenez, C. Maraston, L. Verde, D. Thomas, A. Citro, R. Tojeiro, and D. Wilkinson, “A 6% measurement of the hubble parameter at $z = 0.45$: direct evidence of the epoch of cosmic re-acceleration,” *Journal of Cosmology and Astroparticle Physics*, vol. 2016, no. 05, pp. 014–014, 2016.
- [48] M. Moresco, L. Verde, L. Pozzetti, R. Jimenez, and A. Cimatti, “New constraints on cosmological parameters and neutrino properties using the expansion rate of the universe to $z = 1.75$,” *Journal of Cosmology and Astroparticle Physics*, vol. 2012, no. 07, p. 053, 2012.
- [49] M. Moresco, A. Cimatti, R. Jimenez, L. Pozzetti, G. Zamorani, M. Bolzonella, J. Dunlop, F. Lamareille, M. Mignoli, H. Pearce, *et al.*, “Improved constraints on the expansion rate of the universe up to $z = 1.1$ from the spectroscopic evolution of cosmic chronometers,” *Journal of Cosmology and Astroparticle Physics*, vol. 2012, no. 08, pp. 006–006, 2012.
- [50] M. Smith, C. B. D’Andrea, M. Sullivan, A. Möller, R. Nichol, R. Thomas, A. Kim, M. Sako, F. Castander, A. Filippenko, *et al.*, “First cosmology results using supernovae ia from the dark energy survey: Survey overview, performance, and supernova spectroscopy,” *The Astronomical Journal*, vol. 160, no. 6, p. 267, 2020.
- [51] C. Roberts, K. Horne, A. O. Hodson, and A. D. Leggat, “Tests of Λ cdm and conformal gravity using grb and quasars as standard candles out to $z \sim 8$,” *arXiv preprint arXiv:1711.10369*, 2017.
- [52] M. Demianski, E. Piedipalumbo, D. Sawant, and L. Amati, “Cosmology with gamma-ray bursts-ii. cosmography challenges and cosmological scenarios for the accelerated universe,” *Astronomy & Astrophysics*, vol. 598, p. A113, 2017.
- [53] A. G. Riess, W. Yuan, L. M. Macri, D. Scolnic, D. Brout, S. Casertano, D. O. Jones, Y. Murakami, G. S. Anand, L. Breuval, *et al.*, “A comprehensive measurement of the local value of the hubble constant with 1 km s $^{-1}$ mpc $^{-1}$ uncertainty from the hubble space telescope and the sh0es team,” *The Astrophysical journal letters*, vol. 934, no. 1, p. L7, 2022.
- [54] W. Handley, M. Hobson, and A. Lasenby, “Polychord: nested sampling for cosmology,” *Monthly Notices of the Royal Astronomical Society: Letters*, vol. 450, no. 1, pp. L61–L65, 2015.
- [55] A. Lewis, “Getdist: a python package for analysing monte carlo samples,” *arXiv preprint arXiv:1910.13970*, 2019.
- [56] P. Collaboration, N. Aghanim, Y. Akrami, M. Ashdown, J. Aumont, C. Baccigalupi, M. Ballardini, A. Banday, R. Barreiro, N. Bartolo, *et al.*, “Planck 2018 results. vi. cosmological parameters,” 2020.
- [57] R. C. Nunes, S. K. Yadav, J. Jesus, and A. Bernui, “Cosmological parameter analyses using transversal bao data,” *Monthly Notices of the Royal Astronomical Society*, vol. 497, no. 2, pp. 2133–2141, 2020.
- [58] R. C. Nunes and A. Bernui, “Bao signatures in the 2-point angular correlations and the hubble tension,” *The European Physical Journal C*, vol. 80, pp. 1–8, 2020.
- [59] L. Verde, J. L. Bernal, A. F. Heavens, and R. Jimenez, “The length of the low-redshift standard ruler,” *Monthly Notices of the Royal Astronomical Society*, vol. 467, no. 1, pp. 731–736, 2017.
- [60] T. Lemos, Ruchika, J. C. Carvalho, and J. Alcaniz, “Low-redshift estimates of the absolute scale of baryon acoustic oscillations,” *The European Physical Journal C*, vol. 83, no. 6, p. 495, 2023.